THE COMPANY OF
Biologists

RESEARCH ARTICLE

Histone H3.3 regulates dynamic chromatin states during spermatogenesis

Benjamin T. K. Yuen[1,2,3], Kelly M. Bush[1,2,3], Bonnie L. Barrilleaux[1,2,3], Rebecca Cotterman[1,2,3] and Paul S. Knoepfler[1,2,3,*]

ABSTRACT

The histone variant H3.3 is involved in diverse biological processes, including development, transcriptional memory and transcriptional reprogramming, as well as diseases, including most notably malignant brain tumors. Recently, we developed a knockout mouse model for the *H3f3b* gene, one of two genes encoding H3.3. Here, we show that targeted disruption of *H3f3b* results in a number of phenotypic abnormalities, including a reduction in H3.3 histone levels, leading to male infertility, as well as abnormal sperm and testes morphology. Additionally, null germ cell populations at specific stages in spermatogenesis, in particular spermatocytes and spermatogonia, exhibited increased rates of apoptosis. Disruption of *H3f3b* also altered histone post-translational modifications and gene expression in the testes, with the most prominent changes occurring at genes involved in spermatogenesis. Finally, *H3f3b* null testes also exhibited abnormal germ cell chromatin reorganization and reduced protamine incorporation. Taken together, our studies indicate a major role for H3.3 in spermatogenesis through regulation of chromatin dynamics.

KEY WORDS: Epigenetics, Fertility, Germ cells, Histone variant H3.3, Spermatogenesis, Chromatin, *H3f3b*

INTRODUCTION

During spermatogenesis, a complex interplay of histone post-translational modifications (PTMs) take place in the nuclei of immature germ cells as they develop into mature spermatozoon (Chen et al., 1998; Godmann et al., 2007; Lewis et al., 2003; Payne and Braun, 2006; Rathke et al., 2013; Tachibana et al., 2007; van der Heijden et al., 2006; Zheng et al., 2008). Together with such histone PTMs, histone variants play a major role in the protamine transition and chromatin reorganization process during spermatogenesis, and many histone variants of histone H1 (H1t, H1T2 HILS1), H2A and H2B (TH2A, TH2B, ssH2B, H2A.B.bd, H2BL1, H2BL2, H2AL1-H2AL3) and H3 (H3t, H3.3) become expressed in specific germ cell types or are testes-specific (Lewis et al., 2003; Rathke et al., 2013). The N-terminal tail of H3 acquires specific PTMs during spermatogenesis, including methylation of residue Lys9, a mark involved in chromatin condensation and gene repression, although other residues, such as Lys27 of H3 and Lys20 of H4 also undergo PTM and play roles in establishing repressive chromatin (Jenuwein and Allis, 2001; Kouzarides, 2007; Payne and Braun, 2006). Aberrant

regulation of H3 PTMs leads to germ cell apoptosis, defective spermiogenesis and infertility (Iwamori et al., 2011; Liu et al., 2010; Okada et al., 2007; Peters et al., 2001; Tachibana et al., 2007).

Histone variant H3.3 is encoded by two genes in *Mus*, *H3f3a* and *H3f3b*, although both *H3f3a* and *H3f3b* transcripts contain divergent 5′- and 3′-untranslated regions and regulatory sequences that mediate at least partially distinct expression patterns (Akhmanova et al., 1995; Szenker et al., 2011; Witt et al., 1997). H3.3 is incorporated into chromatin in transcriptionally active regions undergoing nucleosome displacement; this is in contrast to the canonical histone H3.1 and H3.2 proteins, which are deposited into chromatin in a replication-dependent manner (Ahmad and Henikoff, 2002; Ray-Gallet et al., 2011; Tagami et al., 2004). This difference is due in part to the unique structure of H3.3, which differs from H3.1 and H3.2 by five and four amino acids, respectively. Of particular importance, H3.3 contains unique Ala87, Ile89 and Gly90 residues, which grant H3.3 the ability to destabilize nucleosomes in transcriptionally active regions (Ahmad and Henikoff, 2002; Jin et al., 2009).

Loss of H3.3 through disruption of either *H3f3a* or *H3f3b* causes defects in fertility (Bush et al., 2013; Couldrey et al., 1999; Hodl and Basler, 2009; Sakai et al., 2009; Tang et al., 2013). H3.3 is expressed throughout the mouse seminiferous tubule (Bramlage et al., 1997) and accumulates in the sex body of spermatocytes (van der Heijden et al., 2007). H3.3 is also not completely removed from chromatin during spermiogenesis (Erkek et al., 2013; Hammoud et al., 2009), and the relatively small remaining H3.3 fraction is enriched in genomic regions important for zygotic development, potentially transmitting a parental epigenetic memory between generations (Erkek et al., 2013; Hammoud et al., 2009). Thus, H3.3 appears to play a crucial role in male spermatogenesis, although the cellular and molecular mechanisms by which H3.3 influences fertility largely remain an open question.

We recently generated an *H3f3b* null mouse model (Bush et al., 2013). Surviving *H3f3b* null males (hereafter referred to as null) displayed complete infertility. Here, we explore the mechanisms involved in the male infertility phenotype. Null male mice have abnormal testes and sperm morphology. Null males also exhibit increased rates of apoptosis in specific germ cell populations and in sperm, and aberrant levels of histone PTM and spermatogenesis-related gene expression within the testes. Finally, null testes display defective germ cell chromatin reorganization and a failure of normal protamine incorporation. These studies overall indicate that H3.3 plays an important role in regulating chromatin states, which are involved in proper male mouse germ cell development.

RESULTS

Loss of *H3f3b* in testes disrupts normal H3.3 deposition during spermatogenesis

To examine the extent of H3.3 histone protein reduction upon homozygous targeted disruption of *H3f3b*, we first examined

[1]Department of Cell Biology and Human Anatomy, Shriners Hospital For Children Northern California, Sacramento, CA 95817, USA. [2]Genome Center, University of California Davis School of Medicine, Shriners Hospital For Children Northern California, Sacramento, CA 95817, USA. [3]Institute of Pediatric Regenerative Medicine, Shriners Hospital For Children Northern California, Sacramento, CA 95817, USA.

*Author for correspondence (knoepfler@ucdavis.edu)

DEVELOPMENT

whole-testes cell lysate (WTCL). Loss of *H3f3b* did not lead to significant changes in total H3 levels in WTCL (supplementary material Fig. S1A,B) but resulted in a >2-fold reduction in H3.3 protein levels (supplementary material Fig. S1C-E, *P*=0.005), similar to previous reports following *H3f3b* loss in mouse embryonic fibroblasts (MEFs) (Bush et al., 2013). Notably, several faint, but consistently higher molecular-mass H3.3 bands were evident in wild-type (WT) samples but not in those from null mice (supplementary material Fig. S1C,D), indicating the involvement of larger, uncharacterized H3.3-specific PTMs in testes, because these PTMs were not observed in other cell types.

H3f3a transcripts are expressed throughout the testes (spermatogonia, spermatocytes and spermatids) at low levels, whereas *H3f3b* is most highly expressed specifically in spermatocytes (Bramlage et al., 1997). We utilized an H3.3-specific antibody for immunohistochemistry-based immunofluorescence staining (IHC-IF) in mouse testes sections from *H3f3b* WT and null male animals, along with a lectin peanut agglutinin (lectinPNA) conjugate that recognizes the sperm acrosome used to stage-match testes cross-sections (Aviles et al., 1997; Szasz et al., 2000). H3.3 protein accumulated in the nuclei of spermatogonia and leptotene spermatocytes (Fig. 1A,B) in WT tubules. Nuclear H3.3 levels peaked during mid-stage in WT pachytene spermatocytes and persisted throughout meiosis and most of spermiogenesis, with H3.3$^+$ focal regions appearing within the nuclear interior of WT pachytene and diplotene spermatocytes (Fig. 1A,C; supplementary material Fig. S1F, G), corresponding to regions resembling the sex body (van der Heijden et al., 2007). WT step 1-8 round spermatids expressed H3.3 throughout the nucleus and at bright focal points within the nuclear interior, most likely to be the sex body described previously in *Mus* (van der Heijden et al., 2007) (supplementary material Fig. S1F,G). Relative H3.3 levels began to decrease in step 11 WT elongating spermatids (Fig. 1C) and were undetectable in step 12-16 spermatids (supplementary material Fig. S1F,G).

As expected, null tubules displayed substantially lower levels of H3.3 by IHC-IF analyses. H3.3 was nearly undetectable in spermatogonia, pre-leptotene, leptotene, zygotene and early pachytene (stage I-II) spermatocytes in null tubules. Faint nuclear expression of H3.3 became apparent in mid-stage (stage IV-V) null spermatogonia (supplementary material Fig. S1F) as opposed to those of WT, in which H3.3 expression was first detected in early spermatogonia populations. Weak nuclear focal expression of H3.3 was seen in early- to mid-stage null pachytene spermatocytes (stage III-V, supplementary material Fig. S1F,G), but the diffuse nuclear staining was never comparable in intensity to that observed in WT. Nuclear and focal areas of H3.3 protein localization in step 1-11 spermatids were also substantially fainter in null testes, and H3.3 was undetectable by IHC-IF in step 12-16 spermatids. Thus, knockout of *H3f3b* results in substantial decreases in H3.3 protein levels throughout spermatogenesis in a number of cell types within the seminiferous tubule (supplementary material Fig. S2), with the remaining low levels of H3.3 produced from *H3f3a*.

Loss of *H3f3b* leads to male testes atrophy and decreased germ cell types

We examined WT and surviving null mature male mice (supplementary material Fig. S3 and Table S1 for age ranges, *P*=0.420) for defects. Nulls possessed smaller testes, both when compared with their WT littermates and when normalized to animal mass (supplementary material Fig. S3A-E). Compared with WT testes histological sections (supplementary material Fig. S3F), null seminiferous tubules exhibited abnormal architecture, with small and unusually open tubules and reduced numbers of germ cell types and early spermatozoa.

To determine the effect of *H3f3b* loss on spermatid quantity within a tubule cross-section, we measured the number of stage I round (step 1) and elongated (step 13) spermatids in WT and null tubules. Step 1 round spermatids are the direct result of meiotic divisions in spermatocytes that take place in the preceding stage XII tubules. We observed a significant 1.46-fold decrease in the total number of
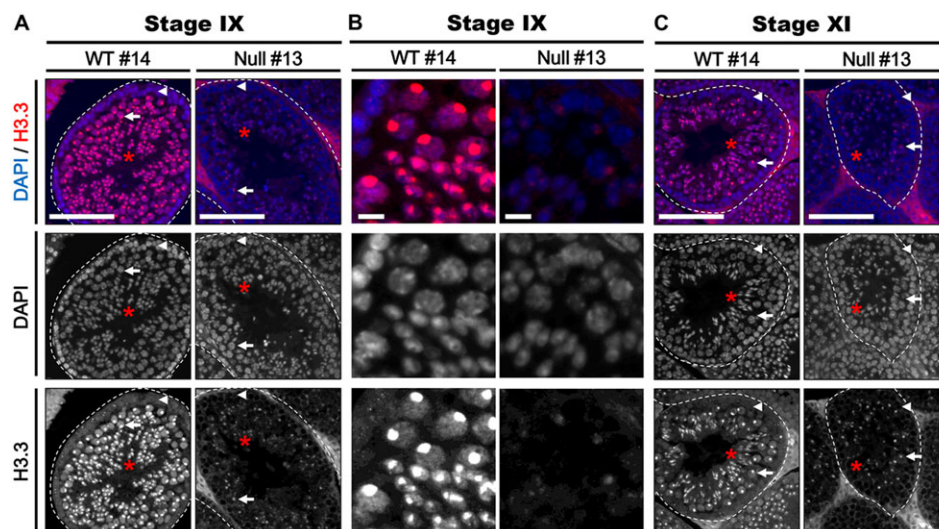
Fig. 1. Alterations of the normal levels and patterns of H3.3 protein in *H3f3b* null testes. Immunohistochemistry staining of WT and null testes sections. (A) H3.3 (red) protein is present in WT stage IX tubules in spermatogonia and leptotene spermatocytes (white arrowhead), in pachytene spermatocytes (white arrow) and in elongating spermatids (red star). Null tubules show little or no H3.3 staining in spermatogonia and leptotene spermatocytes at this stage, and H3.3 is only weakly evident in pachytene and elongating spermatids. (B) Higher magnification images more clearly show considerable reductions in H3.3 staining in null stage IX spermatocytes and elongating spermatids. (C) H3.3 is strongly expressed in WT diplotene spermatocytes (white arrow) and weakly in elongated spermatids (red star) and in zygotene spermatocytes (white arrowhead). Null tubules exhibit weak focal H3.3 protein in diplotene spermatocytes and elongated spermatids, with no nuclear H3.3 staining. H3.3 was nearly undetectable in zygotene spermatocytes in null tubules. DAPI (blue) was used for counterstaining. Scale bars 100 μm (A,C); 10 μm (B). White dotted lines indicate borders of specified tubule. Staining was performed using *n*=2 WT and *n*=4 null animals.

spermatids per null tubule area (supplementary material Fig. S3G), comprising a 1.36-fold decrease in round spermatids and a 1.6-fold decrease in elongated spermatids at this stage (supplementary material Fig. S3H,I). In order to further investigate potential changes in germ cell quantity, we used fluorescence-activated cell sorting (FACS) based on previously established protocols (Bastos et al., 2005; Gaysinskaya et al., 2014; Getun et al., 2011) on testes from two WT and four null aged males (see supplementary material Table S1). We utilized FACS to successfully separate spermatogonia, pre-leptotene spermatocytes, spermatocytes and spermatids with a high degree of enrichment (supplementary material Fig. S4A-H). The FACS profiles of WT and null populations showed high similarity in cell type distribution, although null testes contained substantially fewer cells overall (supplementary material Fig. S5A,B). Null testes exhibited comparable populations of spermatogonia and spermatocytes (supplementary material Fig. S5C,D) and a slight but significant increase in spermatid number (supplementary material Fig. S5E, P=0.033). These data suggest that despite the observed decrease in spermatid numbers per tubule cross-section, the overall proportion of spermatids in relation to other germ cell types is similar to that of WT. Null testes also exhibited a 1.9-fold decrease in the number of pre-leptotene spermatocytes (supplementary material Fig. S5F, P=0.020), indicating increased cell death in this population, or fewer spermatogonia transitioning into this cell type.

Loss of *H3f3b* has been reported to cause defects in chromosome segregation (Bush et al., 2013). We quantified the number of stage XII meiotic tubules in WT and null testes to determine whether *H3f3b* loss leads to a higher preponderance of stalled meiotic tubules by utilizing immunostaining of phosphorylated residue Ser10 on H3 (H3 S10P), a marker of mitotic and meiotic cells (Korhonen et al., 2011). Null testes exhibited a slight, but non-significant, increase in the proportion of meiotic tubules per absolute number of seminiferous tubules (12.3%) compared with WT (10.7%) (supplementary material Fig. S6A). We did not detect a difference in the number of meiotically dividing cells within a tubule when normalized to the tubule area (supplementary material Fig. S6B, P=0.923). Removal of *H3f3b* was previously shown to affect Cenpa incorporation and possibly contribute to centromere dysfunction in MEFs (Bush et al., 2013). We did not observe an increase in the number of Cenpa[+] foci per spermatogonia or spermatocyte in null tubules (supplementary material Fig. S6C,D). These findings suggest that the observed changes in spermatid populations are not likely to result from defective meiotic processes.

H3f3b null males exhibit reduced sperm concentration, abnormal sperm morphology and apoptotic events in spermatocyte and spermatogonia cell types

To further explore the mechanisms of *H3f3b* null male infertility, we analyzed the sperm of WT-control and null males (Table 1). Null males exhibited >2-fold decrease in total sperm concentration. The null sperm that were present were quite abnormal, exhibiting >2-fold decreases in motility, >3-fold decreases in rapid cells and >4-fold decreases in progressive motility (supplementary material Movies S1, S2). Examination of WT and null sperm under high magnification revealed major abnormalities in morphology (Fig. 2A), with 99% of null sperm having abnormal heads (versus 30% of WT), indicating possible defects in meiotic chromatin condensation (Fig. 2B).

We also examined the potential effects that *H3f3b* loss would have on cell survival in the testes. We observed a 2.06-fold increase in the percentage of apoptotic tubules per null testis (Fig. 2C, classified as exhibiting one or more TUNEL[+] nuclei per tubule) and a 1.63-fold

Table 1. Summary of sperm characteristics in *H3f3b* null mice

Genotype	Concentration (M/ml)	Motile (%)	Progressive movement (%)	Rapid cells (%)
H3f3b WT*	37.00±5.71	72.67±11.86	40.67±10.73	60.33±13.78
H3f3b null*	15.48±2.70	27.00±8.68	9.60±3.41	17.60±5.71
t-test[‡]	$7.96×10^{-3}$	0.020	0.014	0.015
Reference	20-50	>40	>15	>30

Summary of sperm characteristics in *H3f3b* null males. Null males exhibit significantly reduced sperm concentration as well as a reduced percentage of motile sperm, sperm capable of progressive movement and sperm capable of rapid movement. Reference ranges are from UCD Mouse Biology Program.
*Mean±s.e.m.
[‡]Student's two-tailed *t*-test.
Sperm measurements were taken from *n*=3 WT and *n*=5 null animals.

increase in the absolute number of apoptotic tubules per null testis relative to WT (Fig. 2D). Null tubules also exhibited a significant 3.53-fold increase in apoptotic events (4.25% of null cells versus 1.20% of WT) (Fig. 2E). In null testes, the majority of apoptotic events took place in or around stage IX tubules, within one to two cell-layers from the tunica propria, where pre-leptotene spermatocytes transition into leptotene spermatocytes (Fig. 2F; supplementary material Fig. S2, Fig. S7A,D), with few apoptotic nuclei detected in early (stage I-V) and nearly no apoptotic nuclei detected during mid-stage (stage VI-VIII). Null tubules also exhibited very high levels of TUNEL[+] nuclear fragments, which were essentially absent in the WT tubules (Fig. 2F, red stars). Examination of subsequent stages corroborated these findings because stage X tubules also contained increased numbers of apoptotic nuclei one to two cell-layers away from the tunica propria, corresponding to leptotene and pachytene spermatocytes (supplementary material Fig. S7B). Often, TUNEL[+] null tubule sections in the stages following stage IX exhibited small and degraded apoptotic nuclei near the tunica propria, suggesting that these nuclear fragments are the remnants of earlier apoptotic nuclei (supplementary material Fig. S7B,C).

H3f3b deficiency results in sharply elevated H3K9me3 levels in distinct germ cell populations

Because histone PTM plays key roles in spermatogenesis, we sought to determine whether aberrant histone methylation could play a role in the observed defects in *H3f3b* null testes. We utilized IHC-IF to examine the levels of H3 Lys9 trimethylation (H3K9me3), a mark associated with transcriptional silencing and heterochromatin. H3K9me3 levels were strikingly higher overall in null testes when compared with those of WT (supplementary material Fig. S2, Fig. S8A). WT mice exhibited patterns of H3K9me3 staining that were consistent with previous reports of H3K9me3 in normal mouse testes, in which H3K9me3 was found in spermatogonia, pre-leptotene, leptotene and pachytene spermatocytes, and in the chromocenters of round spermatids (Iwamori et al., 2011; Liu et al., 2010; Payne and Braun, 2006). By contrast, in nulls, nuclear H3K9me3 staining was relatively more intense in spermatogonia, pre-leptotene, leptotene, zygotene and early (stage I-V) pachytene spermatocytes (supplementary material Fig. S9, Fig. S10). H3K9me3 levels did gradually decrease from pachytene to diplotene stages of meiotic prophase (Fig. 3A,B), although H3K9me3 levels were still higher in null tubules. H3K9me3 nuclear foci with intensities much higher than those seen in WT persisted in null pachytene spermatocytes and step 1-13 spermatid chromocenters, and null tubules typically exhibited more brightly stained focal points in secondary or meiotic spermatocytes when compared with WT (Fig. 3C).
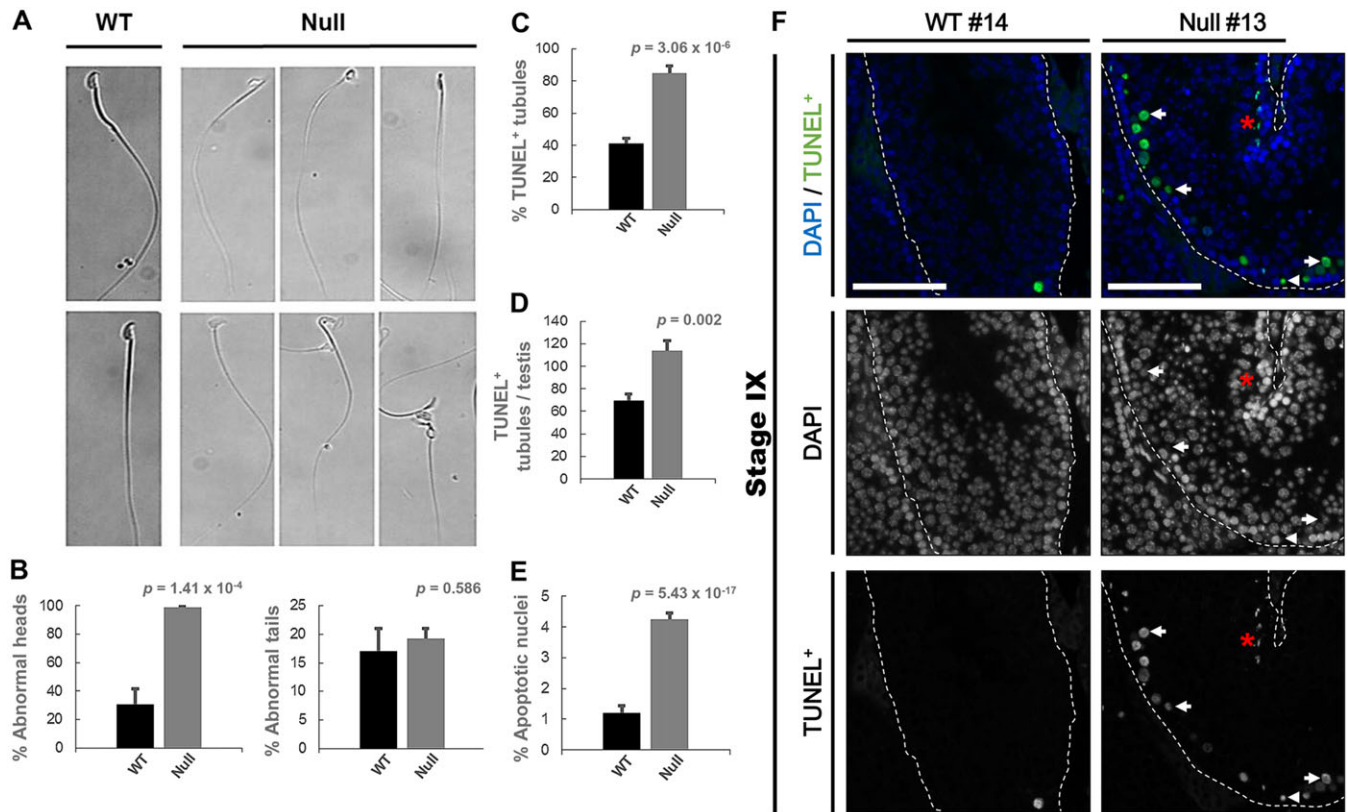
Fig. 2. Gross defects in null sperm and increased germ cell apoptosis upon targeted disruption of *H3f3b*. (A) Sperm from *H3f3b* null animals display abnormal characteristics compared with their WT counterparts. A variety of defects found in null sperm are shown in these representative images. (B) Analysis of sperm. Data presented are means±s.e.m. (C,D) Null testes exhibit a significant 2.06-fold increase in the percentage of apoptotic tubules per testis (C) and a significant 1.63-fold increase in the absolute number of apoptotic tubules per testis (D). (E) Nulls exhibited a 3.5-fold increase in the percent of apoptotic nuclei per tubule. (F) Apoptotic events were primarily detected one to two cell-layers luminally from the tunica propria of the seminiferous tubule. White arrowheads indicate spermatogonia, white arrows indicate leptotene and/or pachytene spermatocytes and red stars indicate regions containing fragmented apoptotic nuclei. DAPI (blue) was used for counterstaining. Scale bars: 100 µm. White dotted lines indicate borders of specified tubule. Sperm measurements were taken from n=3 WT and n=5 null animals. TUNEL staining was performed on n=4 WT and n=6 null animals.

When we enriched for histone-containing chromatin proteins using acid extraction on whole testes, we observed a 1.85-fold increase in the levels of H3K9me3 relative to those of total H3 by immunoblotting samples from null males (P=0.001, Fig. 3D,E). By contrast, the amount of H3K9me3 relative to β-actin in WTCL from nulls was not elevated (P=0.287, supplementary material Fig. S8B-D). To determine whether H3K9me3 accumulates specifically in the cell types in which we observed TUNEL$^+$ events, we stained pre-leptotene spermatocytes and spermatocytes for H3K9me3. Sorted pre-leptotene spermatocytes exhibited a 1.97-fold higher level of H3K9me3, through IHC-IF analyses, relative to WT (supplementary material Fig. S8E,F, P<0.001). Sorted null spermatocytes and null γH2A.X$^+$ spermatocytes (primarily pachytene cells) generally displayed higher levels of H3K9me3, although this difference was not significant (supplementary material Fig. S8G,H).

To determine whether *H3f3b* loss could affect other PTMs, we also examined levels of the euchromatic Lys4 trimethylation mark on H3 (H3K4me3) and the repressive Lys27 trimethylation mark on H3 (H3K27me3) in WT and null testes. We were able to detect a small, yet consistent decrease in the levels of H3K4me3 in null testes by IHC-IF (supplementary material Fig. S11A) but were unable to discern a difference in specific localization patterns between WT and null tubules. H3K4me3 levels were slightly decreased in null WTCL when compared with that from WT littermates, although overall this decrease was not significant

(supplementary material Fig. S11B,C). H3.3 is enriched for euchromatic marks, such as H3K4me3 (Hake et al., 2006; McKittrick et al., 2004), and the observed decreases could reflect a loss of H3K4me3-bearing H3.3 histones. We were also unable to detect a significant difference in the amount of H3K27me3 between the two genotypes through analyses of WTCL (supplementary material Fig. S11D) or IHC-IF analyses (data not shown). We observed significant increases in the relative phosphorylation levels of the H3.3-specific Ser31 residue (H3.3 S31P) in null testes (supplementary material Fig. S11D, compared with the total H3.3 protein levels in the same samples shown in supplementary material Fig. S1C-E), suggesting that the remaining H3.3 protein in nulls might become hyper-phosphorylated on Ser31, as described previously (Bush et al., 2013). Notably, H3.3 S31P was found to localize primarily to meiotically dividing spermatocytes in stage XII tubules (supplementary material Fig. S11E) in samples from both WT and null mice. These results suggest that loss of H3.3 primarily affects H3K9me3 PTM at specific timepoints in spermatogenesis, particularly during the pre-leptotene to leptotene transition.

H3f3b loss disrupts the expression of crucial spermatogenesis-related genes

We isolated RNA from *H3f3b* WT and null testes and conducted gene expression microarray studies. Employing a 2-fold or greater expression change cutoff, only six genes were up- or downregulated
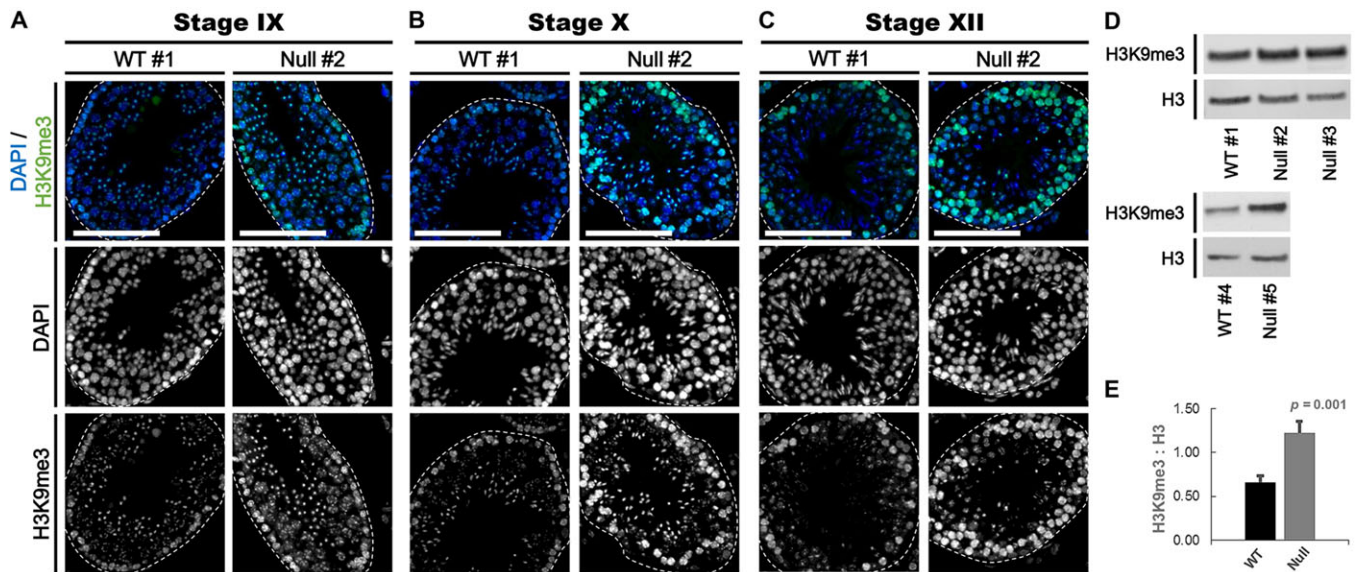
Fig. 3. Histone H3.3 influences H3K9me3 levels in late-stage tubules. Immunohistochemistry staining for H3K9me3. (A) The H3K9me3 (green) signal was strongest in null spermatogonia, leptotene spermatocytes and focal points in elongating spermatids, and was diffuse in pachytene spermatocytes. (B) The H3K9me3 levels in stage X tubules were strongest in null spermatogonia and leptotene spermatocytes, but were weaker along the tubule lumen in pachytene spermatocytes and elongating spermatids. (D) H3K9me3 staining was strongest in spermatogonia and zygotene spermatocytes, with weak focal staining of meiotic spermatocytes and spermatids in stage XII null tubules. (D) Null males demonstrated increased H3K9me3 levels relative to the total H3 levels in nuclear acid extracts. (E) Nulls exhibit a 1.85-fold increase in the H3K9me3:H3 ratio (P=0.001). DAPI (blue) was used for counterstaining. Scale bars: 100 μm. White dotted lines indicate borders of specified tubule. H3K9me3 staining was performed on n=4 WT and n=6 null animals.

by loss of *H3f3b,* with one of the downregulated genes being *H3f3b* itself (supplementary material Table S2). Using a 1.5-fold cutoff, 186 and 375 genes in total were up- and downregulated in testes by loss of *H3f3b*, respectively (supplementary material Table S3). Importantly, the expression changes in 45 of the up- and 111 of the downregulated genes were shared events in both samples from null mice (supplementary material Table S3). Database for annotation, visualization and integrated discovery (DAVID) gene ontology (GO) analysis (Huang et al., 2009a,b) revealed that the most prominent ontological cluster of genes downregulated using the 1.5-fold cutoff were genes associated with sperm and spermatogenesis. These genes included *Catsper1* and *Catsper3* (cation channel, sperm associated 1 and 3), *Spaca3* and *Spaca4* (sperm acrosome 3 and 4), the flagellum associated gene *Cabyr*, the spermatozoa associated *Hook1* and the spermatogenesis-linked adipogenin (*Adig*) related cDNA (*BC054059*). Validation quantitative (q) PCR measurements of *Catsper1*, *Spaca3*, *Adig/BC054059* and *Hook1* levels confirmed that these fertility-linked genes were significantly decreased in null adult testis relative to that of WT littermates (Fig. 4A). GO analysis of expression data also indicated that genes found to be upregulated in the null testes were ontologically enriched for an 'induction of apoptosis' functional cluster. Downregulated genes tended to be localized away from CpG-rich regions, whereas 61% of upregulated genes trended the opposite way (supplementary material Table S4). Deregulated genes were not enriched on any particular chromosome (supplementary material Table S4).

For a more detailed analysis invoking a cell-type specific component, we utilized mouse transcriptome data from the Gene Expression Omnibus (GEO) database (GSE21749, GSE4193, GSE23119 and GSE21447) to determine the expression pattern of *H3f3b* null up- and downregulated genes in normal, staged germ cell populations, as performed previously (Gaucher et al., 2012; Tan et al., 2011). Importantly, the majority of genes found to be downregulated by 1.5-fold or more in null testes are normally, and predominantly, expressed in round spermatids and moderately in spermatogonia

(Fig. 4B). This pattern is logical given that a large proportion of downregulated genes was enriched for functional processes involving sperm development. By contrast, the majority of genes upregulated by 1.5-fold or greater are normally expressed in spermatogonia and early spermatocyte (pre-leptotene, leptotene, zygotene) populations (Fig. 4C), the same populations of cells that exhibited an increase in apoptotic events upon TUNEL staining, although it is important to note that pre-leptotene spermatocytes were found to be significantly decreased through FACS analysis in the null.

ChIP-seq analysis reveals epigenomic changes in *H3f3b* nulls

We performed ChIP-seq for H3K4me3 in WT and null testes samples (two biological replicates each). Globally, loss of reads mapping to the *H3f3b* locus was apparent in both null samples, validating the null genotype (supplementary material Fig. S12A). Both null samples had fewer H3K4me3 peaks than both WT samples, and the peaks were on average narrower in null samples than those of WT (supplementary material Table S5). We constructed consensus peak sets for WT and null samples by intersecting the peaks of each replicate. The WT consensus peak set contained 27% more H3K4me3 peaks than the null consensus peak set (Fig. 4D), and the WT peaks were an average of 39% broader than the peaks of the null samples (1680 versus 1210 bp, P<0.0001, supplementary material Fig. S12B). Nearly all of the peaks in the null samples were also found in the WT samples (97%), whereas 23% of the WT consensus peaks were absent from the null consensus peak set. The two WT samples were very similar to each other, with ~90% overlapping peaks (supplementary material Fig. S12C). However, null samples were more divergent; only 81% of the peaks from null sample 73 were also found in null sample 67 (supplementary material Fig. S12D). We used the R package 'DiffBind' to cluster the ChIP-seq data and determine the correlation between samples. WT samples were highly similar to each other (correlation>0.94), whereas the null samples, although
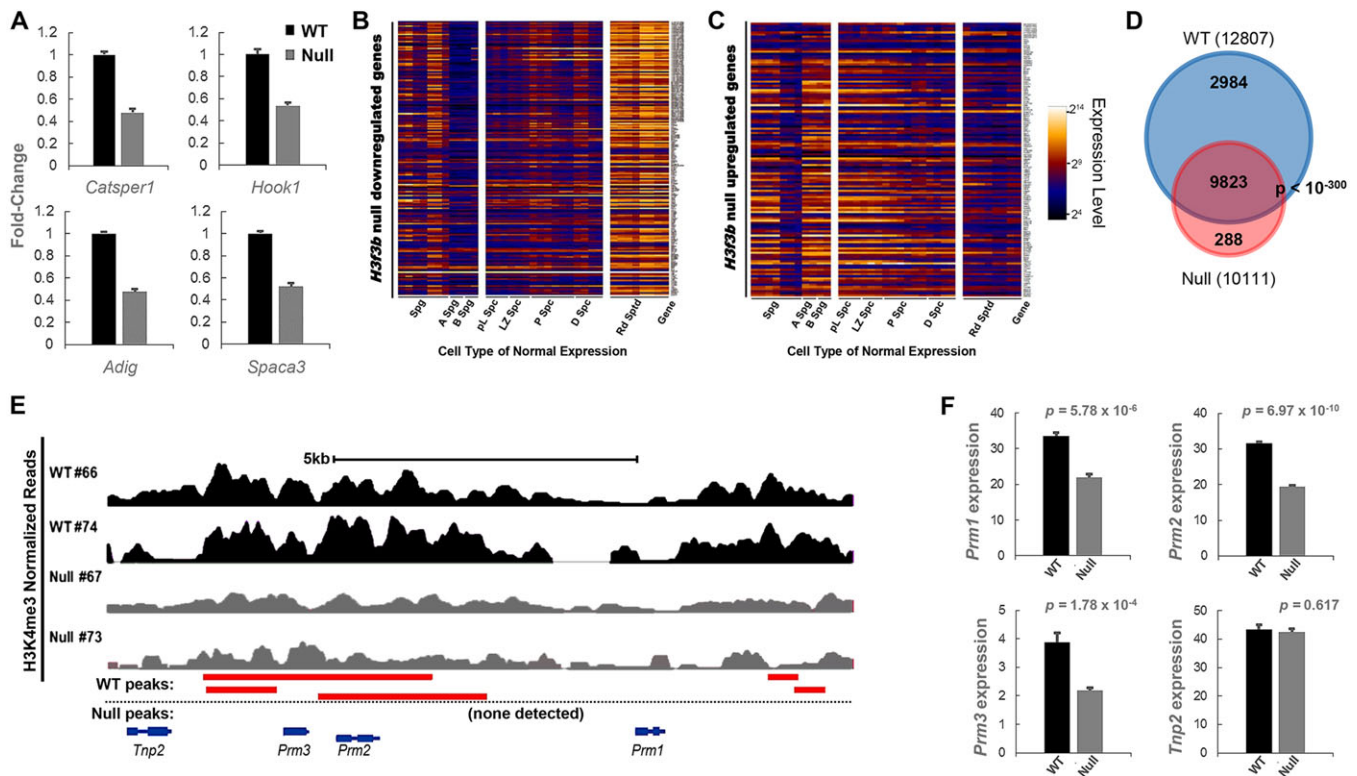
Fig. 4. The influence of H3.3 on transcriptional processes and H3K4me3 within the testes. (A) qPCR analysis for fertility related genes *Catsper1*, *Spaca3*, *Adig/ BC054059* and *Hook1*. Error bars indicate s.d. (B) Genes downregulated, upon array analysis, in null testes are normally expressed in round spermatids, with moderate expression in spermatogonia. Spermatogonia (Spg), A-type Spg (A Spg), B-type Spg (B Spg), pre-leptotene spermatocyte (pL Spc), leptotene/zygotene spermatocyte (LZ Spc), pachytene spermatocyte (P Spc), diplotene spermatocyte (D Spc) and round spermatids (Rd Sptd) array sample columns are shown. (C) Upregulated null genes are expressed normally in spermatogonia and early spermatocyte populations. (D) WT and null samples exhibit a high degree of consensus H3K4me3 peak set overlap using ChIP-Seq analysis. Numbers in parentheses indicate the total number of peaks in each cell type. (E) Compared with WT (black), null (gray) testes display reduced H3K4me3 ChIP-seq peaks around the protamine domain, with a specific loss of peaks around *Prm1-Prm3* and *Tnp2*. Peaks called by HOMER are shown as red bars below. (F) qPCR analyses of whole testes RNA reveals significant decreases in *Prm1-Prm3*, but not *Tnp2* expression in *H3f3b* nulls.

similar in an absolute sense, were relatively less alike to each other (correlation<0.90). The two null replicate samples specifically clustered together, as did the two WT samples with each other, demonstrating that loss of *H3f3b* might result in both overlapping, but also distinct gene expression changes (supplementary material Fig. S13A). DiffBind identified 281 peaks that were significantly reduced in null samples, and 90 peaks that were significantly increased in null samples compared with those of WT (supplementary material Table S6). No consistent pattern of changes in the frequency of satellite repeats were observed in the nulls (supplementary material Fig. S13B).

H3K4me3 peaks increased in null were enriched for embryonic development genes, whereas the decreased peaks were enriched for spermatogenesis genes (supplementary material Tables S6, S7). We found a significant overlap between differentially regulated genes in the nulls that were identified by microarray analyses and genes exhibiting unique or increased and/or decreased patterns of H3K4me3 through ChIP-seq analyses in the nulls (supplementary material Fig. S14A-D). qPCR analyses of overlapping genes between the microarray and H3K4me3 ChIP-seq datasets verified that changes in transcription were reflected in the upregulation or gain of H3K4me3 peaks (supplementary material Fig. S13C-E) or the downregulation or loss of peaks (supplementary material Fig. S13F-H). Notably, both null samples exhibited a loss of H3K4me3 peaks around the protamine domain cluster, comprising protamine genes 1, 2 and 3 (*Prm1-Prm3*) and transition protein

gene 2 (*Tnp2*) (Martins and Krawetz, 2007) (Fig. 4E), and around the transition protein 1 gene (*Tnp1*) (supplementary material Fig. S15A). qPCR analyses on RNA from whole testes revealed significant decreases in *Prm1-Prm3* expression in nulls (Fig. 4F) but surprisingly not in *Tnp1* and *Tnp2* expression (Fig. 4F; supplementary material Fig. S15B), although these results might be affected by differences in germ cell content.

To further explore a loss of expression from the protamine domain cluster in nulls, we examined WT and null spermatids, which had been sorted using FACS. Combined null samples exhibited lower levels of *Prm1* and *Prm2* when compared with combined WT samples (supplementary material Fig. S15C,D), although these differences were not statistically significant. This might be due, in part, to the presence of one outlier null male that exhibited aberrantly high levels of these transcripts (supplementary material Fig. S15E,F). All null males expressed lower levels of *Prm3* ($P=0.030$) and *Tnp2* ($P<0.001$) (supplementary material Fig. S15G,H). Null males did not differ from WT in *Tnp1* expression (supplementary material Fig. S15I). Taken together, these data suggest that H3.3 is necessary for the appropriate expression of spermatogenesis-related genes.

H3f3b knockout leads to asynchronous spermatid development during spermiogenesis

We stained testes sections with lectinPNA to follow acrosome development and spermiogenesis in *H3f3b* WT and null tubules.

Null and WT seminiferous tubules were capable of producing acrosomal granules and an acrosomal cap. However, during spermiogenesis, late-stage null tubules displayed asynchronous spermatid elongation. As the abnormal, mixed nature of late-stage null tubules made it difficult to distinguish stage IX tubules from stage X tubules, we classified stage IX as tubules in which the majority of the spermatids were step 9, whereas those at stage X were characterized as containing a majority of step 10 spermatids among a mixture of step 9-11 spermatids in the tubule lumen. Individual sections of late-stage null tubules frequently exhibited spermatids characteristic of a number of different stages.

Stage IX null tubules consistently exhibited aberrant mixed characteristics of (1) late stage VIII tubules, in which spermatozoa have exited the tubule lumen during spermiation and round spermatids persist, and (2) stage X tubules, in which early elongating spermatids begin to become bilaterally flattened (Fig. 5A). Similarly, stage X null tubules, normally containing bilateral flattening spermatids, frequently exhibited characteristics of stage IX and late-stage tubules (e.g. stage XI) (Fig. 5B), a phenotype that was only very rarely present in WT testes. These data suggest that null tubules do not exhibit synchronized chromatin reorganization, which is normally observed during spermiogenesis. It is also possible that this asynchronous development could lead to elevated spermatid numbers during certain stages of spermatogenesis due to delayed spermiation.

H3f3b is required for the switch from histone- to protamine-based chromatin

Tnp1 plays a key role in the transition to protamine-based chromatin that is essential for normal spermatogenesis and fertility (Balhorn, 2007; Braun, 2001; Carrell et al., 2007; Miller et al., 2010; Okada et al., 2007). Tnp1 first becomes strongly expressed in step 11 spermatids (Zhao et al., 2004) and persists until step 13-15 (Yu et al., 2000; Zhao et al., 2004). Null late-stage tubules contained step 8-9 spermatids (Tnp1$^-$) and step 10-11 spermatids (Tnp1$^+$) within the same tubule, an exceedingly rare occurrence in stage-matched WT tubules (supplementary material Fig. S2; Fig. 5C). In addition, Tnp1$^+$ spermatids were abnormally present in a small number of mid-stage null tubules.

To further examine whether H3f3b loss affected chromatin reorganization and proper sperm function by interfering with protamine replacement into chromatin, we stained WT and null testes for Prm1. The highest amount of Prm1 protein staining in WT tubules was found in step 11-16 spermatids (stage XI-VIII tubules) (supplementary material Fig. S2; Fig. 6A,B), as previously reported (Zhao et al., 2004). By contrast, Prm1 staining in step 11-16 null spermatids was dramatically reduced (Fig. 6A,B and supplementary material Fig. S16A,B), perhaps a result of, at least in part, the decrease in total spermatids per tubule area and reduced Prm1 expression. Levels of Prm1 in null tubules was also very weak or undetectable in late, mixed-stage tubules with delayed step 8-9 spermatids present within the luminal area.

Prm1 levels were also decreased in null decondensed sperm (Fig. 6C). Decondensed null sperm also exhibited higher overall levels of H3K9me3 than those of WT (Fig. 6C; supplementary material Fig. S16C) and in a significantly higher proportion of sperm (supplementary material Fig. S16D, $P<0.001$). Null sperm were also found to have a high number of apoptotic nuclei by TUNEL staining (supplementary material Fig. S16C) with 23% of null sperm being TUNEL$^+$, 12.1-fold higher than WT ($P<0.001$, supplementary material Fig. S16E). Increased levels of H3K9me3 in null sperm were moderately correlated to the increase in sperm
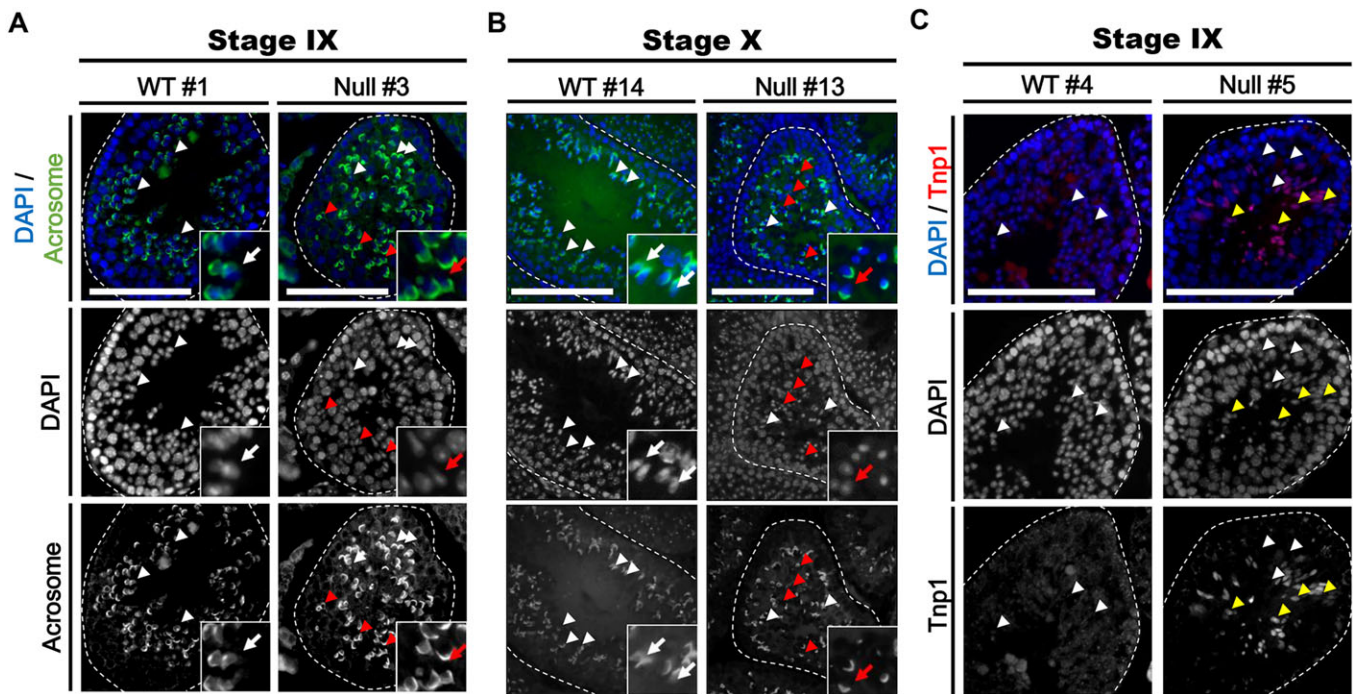
Fig. 5. Knockout of H3f3b causes asynchronous chromatin reorganization. (A) Acrosomal (green) staining indicates that WT stage IX tubules typically exhibit a homogenous, normal population of spermatids beginning elongation (white arrows), whereas null tubules display a mixture of spermatid development (red and white arrows). (B) Stage X WT tubules exhibit bilaterally flattening spermatids (white arrows), whereas null tubules frequently display a mixture of elongating or fully elongated spermatids (red and white arrows). Inset images show magnified areas. (C) WT stage IX tubules do not typically display Tnp1 (red) expression (white arrows); by contrast, null tubules present step 9 (Tnp1$^-$, white arrows) or later (Tnp1$^+$, yellow arrows) in the same tubule. DAPI (blue) was used for counterstaining. Scale bars: 100 µm. White dotted lines indicate borders of specified tubule. Tnp1 staining was performed on n=4 WT and n=5 null animals.
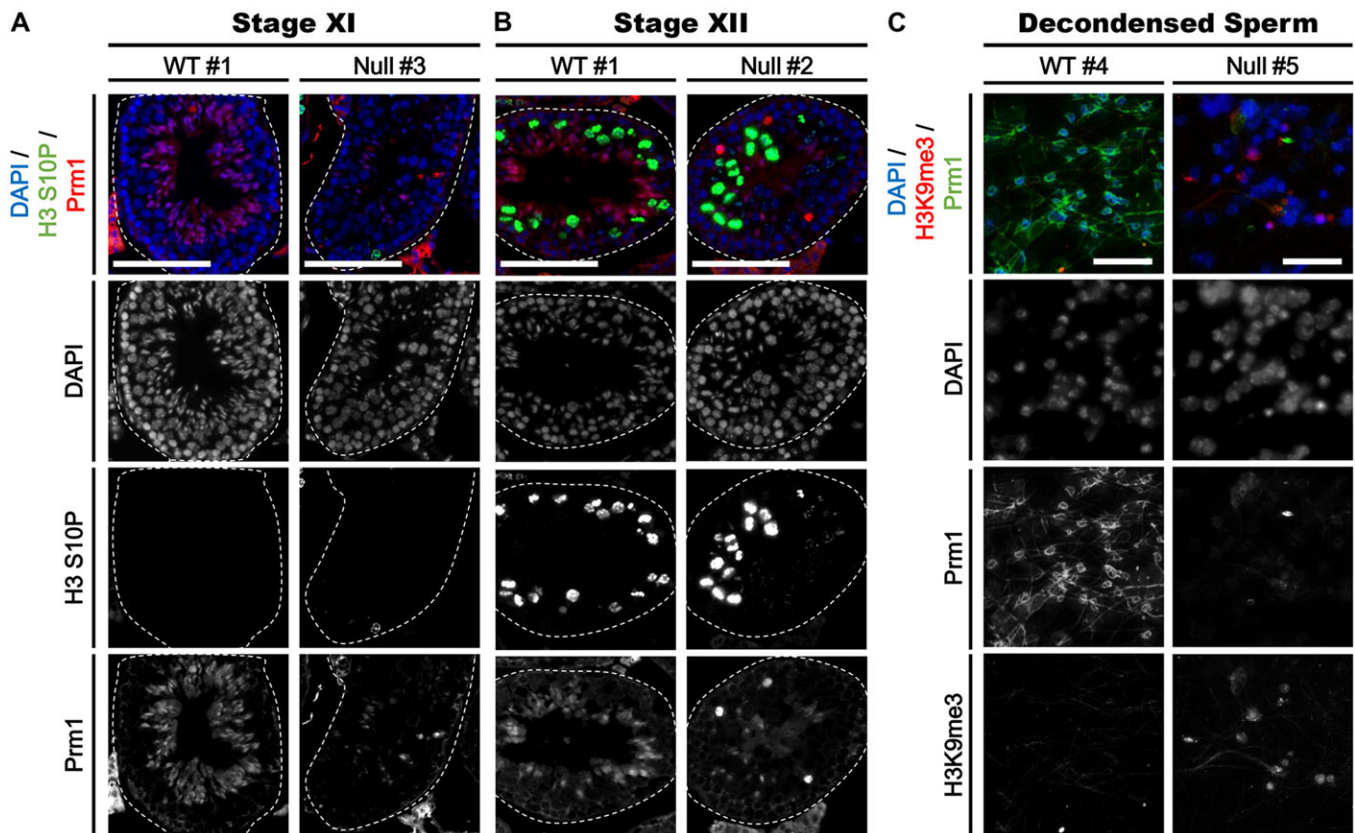
Fig. 6. *H3f3b* is required for appropriate protamine incorporation. (A,B). Immunostaining reveals that Prm1 (red) levels are substantially reduced in null step 11 (A) and step 12 (B) spermatids. H3 S10P (green) staining was used to identify meiotic tubules. (C) Immunostaining of decondensed null sperm demonstrates decreased Prm1 (green) expression and an increase in H3K9me3 (red) expression. DAPI (blue) was used for counterstaining. Scale bars: 100 μm (A,B); 20 μm (C). White dotted lines indicate borders of specified tubule. H3 S10P staining was performed on *n*=2 WT and *n*=3 null animals. Prm1 staining was performed on *n*=3 WT and *n*=4 null animals.

apoptosis, as 18.8% of H3K9me3$^+$ sperm were also TUNEL$^+$ (*P*<0.001, supplementary material Fig. S16F). Taken together, these data indicate that H3.3 is necessary for the switch to protamine-based chromatin and for normal chromatin restructuring during spermatogenesis.

DISCUSSION

Here, we found that reduced H3.3 levels, as a result of *H3f3b* knockout, disrupted male reproductive function through developmental defects, resulting in dysfunctional spermatozoa and reduced total spermatozoa numbers. One possible explanation for the decreased sperm concentration could be defects arising in meiosis, although we were unable to discern significant differences in the number of stage XII meiotic tubules or in the number of meiotically dividing spermatocytes in WT and null testes. However, the null cells with the strongest meiotic defects could well be those most prone to apoptosis and hence be lost for analysis. Another explanation is that reduced sperm levels could be due to elevated levels of apoptosis that are not directly related to meiosis; indeed, a substantial proportion of null epididymal sperm exhibited apoptotic nuclei, suggesting that lethal defects arise as a result of earlier events in the generation of the sperm that are disrupted in the null.

Notably, the majority of apoptotic events in null testes occurred in or around stage IX (supplementary material Fig. S2), a period where spermatogonia stem cells differentiating into spermatocytes cross the tightly regulated blood-testis barrier (BTB) (Bordlein et al., 2011; Cheng and Mruk, 2012; Morales et al., 2007; Mruk and

Cheng, 2004; Oishi et al., 2004). Downregulated genes in null testes are expressed normally in spermatogonia, a cell type that in null mice also displayed increases in H3K9me3, indicating that an aberrant repressive chromatin state established in the early stages of null spermatogonia development might impede the expression of genes necessary for differentiation into pre-leptotene spermatocytes and the BTB transition.

Strong decreases in H3.3 and increases in H3K9me3 were observed in late-stage null tubules (supplementary material Fig. S2), particularly in spermatogonia and spermatocytes. Western blotting for chromatin-bound H3K9me3 from acid extract revealed a significant increase in levels compared with those of WT. Although this change was not detectable in WTCLs, this discrepancy might be due to the variation in germ cell size within the testes, demonstrated by the fact that the increase of H3K9me3 varied amongst distinct cell types, or because WTCLs include concentrations of non-chromatin bound histones that probably have distinct PTM patterns. A previous study (Okada et al., 2007) has demonstrated that knock out of the histone demethylase Jhdm2a leads to elevated levels of H3K9me3 in round spermatids, although these changes were undetectable using western blot.

H3.3 is normally depleted for H3K9 methylation (Hake et al., 2006; McKittrick et al., 2004) and is thought to inhibit the spread of heterochromatin, in part through eviction of histones carrying H3K9 methylation (Nakayama et al., 2007). Thus, the gains in the amount of H3K9me3 in *H3f3b* null testes cells might be a direct consequence of decreased H3.3 protein. The H3K9me3

DEVELOPMENT

methyltransferase Suv39h2 is most highly expressed in B-type spermatogonia and leptotene spermatocytes and appears to regulate H3K9 methylation at these stages (O'Carroll et al., 2000; Peters et al., 2001), suggesting that the general loss of H3.3 might result in hypermethylation of canonical H3 by Suv39h2. Supporting this hypothesis, H3.3 levels were significantly lower in null germ cell populations where an increased H3K9me3 signal was also observed (supplementary material Fig. S2). Additionally, nucleosome replacement through H3.3 during early pachytene results in a loss of most histone PTMs, leading to the normal *de novo* reappearance of H3K9me3 during stages VI-XII (van der Heijden et al., 2007). We predict that the normal processes by which H3.3 evicts histones bearing repressive PTMs (i.e. H3K9me3) in spermatocytes (Fig. 7A) might be disrupted in null testes, resulting in the overabundance of H3K9me3 (Fig. 7B).

The balance of opened versus closed chromatin during spermiogenesis (Rathke et al., 2013) might also be influenced by H3K9me3, which is involved in chromatin condensation and gene repression (Iwamori et al., 2011; Jenuwein and Allis, 2001; Kouzarides, 2007; Payne and Braun, 2006; Peters et al., 2001). Downregulated genes that are associated with male reproductive function and spermatogenesis in the null testes are normally expressed in round spermatids, suggesting that increased H3K9me3 in round spermatids inhibits their normal development (Fig. 7B). Null sperm also displayed high rates of apoptosis, coinciding with

H3K9me3 expression, indicating that this repressive PTM might aberrantly persist throughout spermiogenesis in null testes, leading to sperm death.

Major replacement of nucleoproteins was also disrupted in null testes (supplementary material Fig. S2), as tubules expressing Tnp1 abnormally exhibited characteristics of both the early- and late-stages of spermiogenesis. Further, Prm1 expression was substantially reduced. Decondensed null epididymal sperm exhibited abnormally high levels of H3K9me3 and low levels of Prm1, suggesting that H3K9me3 inhibits the normal reorganization process by which protamines are incorporated into chromatin. These phenotypic effects in nulls could be a consequence of the lost H3K4me3 peaks around protamine and transition protein genes, the expression of which is essential for proper chromatin condensation and protamine replacement during spermiogenesis (Fig. 7A) (Cho et al., 2003; Lee et al., 1995; Okada et al., 2007). Another possibility is that H3.3 loss and H3K9me3 gain alters nucleoprotein exchange, as disruption of nucleoprotein displacement, particularly in regards to replication-independent histone variants (e.g. TH2B) (Montellier et al., 2013) or histone PTMs (Gaucher et al., 2012), can considerably impact the ability of spermatids to properly condense chromatin and incorporate transition proteins or protamines. In this regard, H3.3 plays an important role in chromatin condensation (Lin et al., 2013). In addition to H3.3, the presence of repressive (e.g. H3K27me3) PTMs and chromatin-
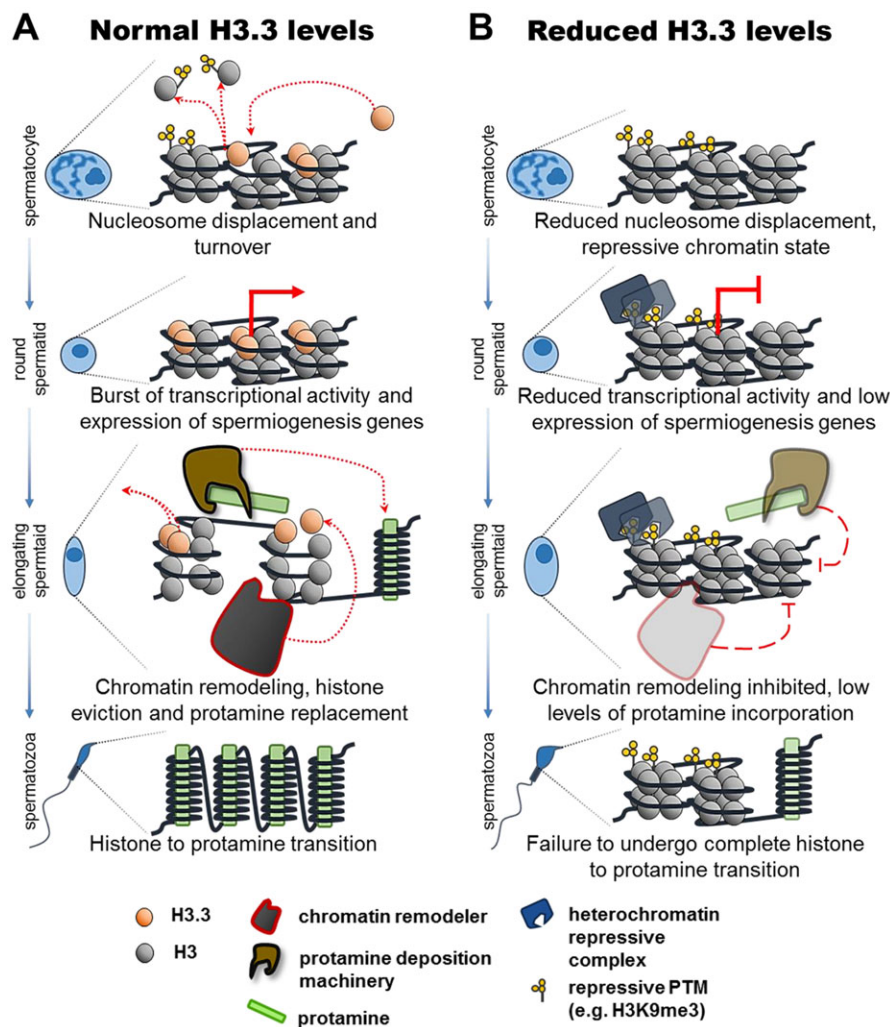
Fig. 7. Model of potential outcomes resulting from H3.3 reduction during spermatogenesis. (A) Normal H3.3 levels allow nucleosome displacement in spermatocytes, resetting many histone PTMs. The presence of sufficient H3.3 also allows for a burst of transcriptional activity in round spermatids, facilitating the transcription of genes required for spermiogenesis, and allows for histone eviction and replacement with protamines. (B) A reduction of H3.3 levels reduces nucleosome turnover in spermatocytes, leading to the accumulation of repressive heterochromatin. Loss of H3.3 also results in lower transcriptional activity and decreased expression of spermiogenesis genes, altering chromatin reorganization dynamics and the transition to protamine.

associated factors contribute to histone retention in protamine-free regions in sperm (Erkek et al., 2013). Taken together, these observations suggest that H3.3 is necessary for normal protamine expression, and further, that the absence of H3.3 and in turn the aberrant presence of repressive PTMs (e.g. H3K9me3) might lead to abnormal chromatin domains in condensing spermatids that block Prm1 deposition in null mice (Fig. 7B).

It is interesting to note that the transcription-coupled incorporation of H3.3 is required to establish marks of active and inactive chromatin that are necessary during fertilization (Erkek et al., 2013); therefore, it might be possible that surviving, null Prm1^{+} spermatozoa face additional problems in activating zygotic transcriptional programs should fertilization occur. The majority of genes with decreased expression were not found in CpG-rich regions, which could suggest that H3.3 plays some regulatory role in maintaining the expression of genes found in CpG-poor areas. Meanwhile, upon H3.3 reduction, the remaining H3.3 histone might be redirected to CpG-rich regions to maintain the function of these genes. Future studies, particularly on *H3f3a*, will further clarify the normal role of histone H3.3 in regulating testes chromatin dynamics and sperm development.

MATERIALS AND METHODS
Animal studies were approved University of California, Davis Institutional Animal Care and Use Committee (IACUC). Additional methods can be found in the supplementary material Methods.

Animals and image analysis
For a comprehensive list of animals used in this study, consult supplementary material Table S1. For a detailed listing on the number of images, cells, testes, or seminiferous tubules used in this study, please consult supplementary material Table S8.

Isolation and immunohistochemistry of testes
Testes (see supplementary material Tables S1, S8) were isolated, embedded in paraffin and specifically treated depending on the antibody (see supplementary material Methods). Primary antibodies against the following proteins were used in this study: H3K9me3 (Abcam 8898), H3K27me3 (Cell Signaling C36B11), H3K4me3 (Millipore 04-745), Tnp1 (Abcam 73135), Prm1 (Briar Patch Biosciences Hup1N), H3 S10P (Millipore 06-570), H3.3 S31P (Abcam ab92628), H3.3 (Abnova H00003021-M01), Sycp3 (from Neil Hunter, UC Davis) and γH2A.X (also from Neil Hunter). Secondary antibodies were used as follows: rabbit or mouse IgG (Alexa488 or Alexa546, Invitrogen) and lectinPNA (Invitrogen L21409). Slides were then mounted using Vectashield mounting medium with DAPI (Vector Labs) and imaged using a Nikon Eclipse 80i microscope (Nikon) with a Retiga 2000R camera (QImaging) or using a Biorevo BZ-9000 microscope system (Keyence).

Testes cell preparation, qPCR and staining analysis for FACS
Testes cell isolation was performed as previously described (Gaysinskaya et al., 2014; Getun et al., 2011) with minor modifications, stained with Hoechst 33342 (Invitrogen #H21492) and propidium iodide (Roche #11348639001), and sorted on a 16 color inFlux v7 high speed cell sorter (Becton-Dickinson-Cytopeia) in a HEPA enclosure. Flow data analysis was performed using FlowJo software (Treestar Incorporated). For qPCR, 75-100% of sorted populations were used for RNA extraction (Macherey-Nagel 740955), concentrated using a Nucleospin RNA XS kit (Macherey-Nagel 740902), and 4-8 ng of RNA was used to amplify cDNA using the CellAmp Whole Transcriptome Amplification Kit (Real Time) Ver. 2 (TaKaRa Biosciences 3734). For staining, sorted cells on slides were treated with antibodies against H3K9me3 (Abcam 8898), Sycp3 and γH2A.X (from Neil Hunter, UC Davis), rabbit or mouse IgG (Alexa488 or Alexa546, Invitrogen), and lectinPNA (Invitrogen L21409) and imaged using a Biorevo BZ-9000 microscope system (Keyence).

WTCL extract, acid extract and western blotting
Whole cell extracts and acid extracts were prepared from one half- to one quarter-testis. Western blotting was performed as described previously (Bush et al., 2013) with a few modifications. Antibodies against the following proteins were used: H3K9me3 (Abcam ab8898), H3K4me3 (Millipore 04-745), β-actin (Sigma A1978), H3.3 (Abnova H00003021-M01), H3.3 S31P (Abcam ab92628), H3K27me3 (Cell Signaling C36B11), H3 (Upstate no. 05-499), anti-rabbit IgG horseradish peroxidase (Jackson 111-035-003), anti-mouse IgG horseradish peroxidase (Jackson 115-035-003), anti-rabbit IgG IRdye800CW (Licor no. 827-08365) and anti-mouse IRdye680RD (Licor no. 926-68170).

qPCR
SYBR Green-based qPCR for genes was performed using Absolute Blue QPCR Master Mix (Thermo Fisher Scientific) and run on a LightCycler 480 (Roche) with included software. Each reaction utilized 10 ng cDNA, and separate reactions containing 10 ng RNA were used to check for genomic DNA contamination. Fold changes were normalized to *Ppia* or *Ubc* and analyzed using the $2^{-\Delta\Delta Ct}$ method.

Microarray and CpG analysis
Microarray analysis was performed on *n*=2 WT and *n*=2 null whole testis RNA extracts, as described previously (Bush et al., 2013). RNA from constitutive *H3f3b* null and WT testes was submitted in biological duplicates. A total of 500 ng RNA from each sample was used on an Illumina MouseWG-6 v2 Expression BeadChip containing over 25,000 probes. Amplification and hybridization were performed at the UC Davis Expression Analysis Core according to the Illumina protocol. The data have been deposited with accession number GSE35303 in the GEO database. For CpG analysis, deregulated gene lists were cross-referenced to CpG island tracks on the UCSC Genome Browser and intersected using Galaxy.

ChIP-seq analysis
We conducted ChIP-seq in WT and null testes tissue using two replicates of H3K4me3 (Millipore 04-745) and matched input controls. Tissue preparation and ChIP were performed as described previously (Barrilleaux et al., 2013). Libraries were prepared as described previously (Bush et al., 2013) and sequenced using an Illumina HiSeq, yielding at least 6 million reads per sample (supplementary material Table S5). The data have been deposited with the accession number GSE60207 in the GEO database.

Seminiferous tubule staging, quantification and Cenpa analysis
Staging of mouse seminiferous tubules was performed as described previously (Ahmed and de Rooij, 2009; Hess and Renato de Franca, 2008; Meistrich and Hess, 2013) using lectinPNA acrosomal staining as a guide. For quantification of meiotic tubules, meiotic spermatocytes and spermatids, testes were stained with an antibody against H3 S10P (Millipore 06-570), lectinPNA (Invitrogen L21409) or lectinPNA alone. Staged tubules were then quantified for the presence of H3 S10P[+] tubules and H3 S10P^{+} cells or round (step 1) and elongated (step 13) spermatids.

Sperm assessment and staining
Male animals were submitted to the UC Davis Mouse Biology Program for sperm functional testing. Sperm were isolated using the swim-out method from the epididymis and assessed using an IVOS computerized sperm analyzer (Hamilton Thorne). Approximately 5×10^6 spermatozoa were placed on slides, decondensed, stained and imaged using a Biorevo BZ-9000 microscope system (Keyence).

TUNEL staining and quantification
Paraffin-embedded testes sections or spermatozoa slides were used for TUNEL staining (DeadEnd Fluorometric TUNEL System, Promega G3250). TUNEL[+] tubules were counted when exhibiting one or more apoptotic events. Quantification of apoptotic nuclei was performed using ImageJ software.

Statistical analysis

Student's two-tailed, unpaired *t*-tests were used to determine significance between null and WT animal measurements. *P*-values for Venn diagram overlaps were calculated in R using the hypergeometric test. Error bars represent s.e.m. unless otherwise noted.

Author contributions

B.T.K.Y. performed the majority of the experiments reported: testes and sperm IHC-IF staining and analysis; sperm imaging and analysis; FACS sorting and analysis; western blotting and quantification; tubule and TUNEL staining, analysis and staging; microarray analysis; CENPA staining and quantification; qPCR; and data preparation and interpretation. K.M.B. performed TUNEL staining, qPCR, the majority of the western blotting, prepared RNA for microarrays, and conducted all mouse breeding and genotyping. B.L.B. performed ChIP-seq data analysis. R.C. prepared ChIP samples. P.S.K. conceived the project, supervised the studies, and along with B.T.K.Y., conducted experimental design and data interpretation. B.T.K.Y. wrote the manuscript. B.T.K.Y., P.S.K., K.M.B., B.L.B. and R.C. read, edited and approved the manuscript.

Supplementary material

Supplementary material available online at
http://dev.biologists.org/lookup/suppl/doi:10.1242/dev.106450/-/DC1

References

Ahmad, K. and Henikoff, S. (2002). The histone variant H3.3 marks active chromatin by replication-independent nucleosome assembly. *Mol. Cell* **9**, 1191-1200.

Ahmed, E. A. and de Rooij, D. G. (2009). Staging of mouse seminiferous tubule cross-sections. *Methods Mol Biol* **558**, 263-77.

Akhmanova, A. S., Bindels, P. C. T., Xu, J., Miedema, K., Kremer, H. and Hennig, W. (1995). Structure and expression of histone H3.3 genes in *Drosophila melanogaster* and *Drosophila hydei*. *Genome* **38**, 586-600.

Aviles, M., Castells, M. T., Martinez-Menarguez, J. A., Abascal, I. and Ballesta, J. (1997). Localization of penultimate carbohydrate residues in zona pellucida and acrosomes by means of lectin cytochemistry and enzymatic treatments. *Histochem. J.* **29**, 583-592.

Balhorn, R. (2007). The protamine family of sperm nuclear proteins. *Genome Biol.* **8**, 227.

Barrilleaux, B. L., Cotterman, R. and Knoepfler, P. S. (2013). Chromatin immunoprecipitation assays for myc and N-myc. *Methods Mol. Biol.* **1012**, 117-133.

Bastos, H., Lassalle, B., Chicheportiche, A., Riou, L., Testart, J., Allemand, I. and Fouchet, P. (2005). Flow cytometric characterization of viable meiotic and postmeiotic cells by Hoechst 33342 in mouse spermatogenesis. *Cytometry A* **65**, 40-49.

Bordlein, A., Scherthan, H., Nelkenbrecher, C., Molter, T., Bosl, M. R., Dippold, C., Birke, K., Kinkley, S., Staege, H. and Will, H. et al. (2011). SPOC1 (PHF13) is required for spermatogonial stem cell differentiation and sustained spermatogenesis. *J. Cell Sci.* **124**, 3137-3148.

Bramlage, B., Kosciessa, U. and Doenecke, D. (1997). Differential expression of the murine histone genes H3.3A and H3.3B. *Differentiation* **62**, 13-20.

Braun, R. E. (2001). Packaging paternal chromosomes with protamine. *Nat. Genet.* **28**, 10-12.

Bush, K. M., Yuen, B. T. K., Barrilleaux, B. L., Riggs, J. W., O'Geen, H., Cotterman, R. F. and Knoepfler, P. S. (2013). Endogenous mammalian histone

H3.3 exhibits chromatin-related functions during development. *Epigenetics Chromatin* **6**, 7.

Carrell, D. T., Emery, B. R. and Hammoud, S. (2007). Altered protamine expression and diminished spermatogenesis: what is the link? *Hum. Reprod. Update* **13**, 313-327.

Chen, H. Y., Sun, J.-M., Zhang, Y., Davie, J. R. and Meistrich, M. L. (1998). Ubiquitination of histone H3 in elongating spermatids of rat testes. *J. Biol. Chem.* **273**, 13165-13169.

Cheng, C. Y. and Mruk, D. D. (2012). The blood-testis barrier and its implications for male contraception. *Pharmacol. Rev.* **64**, 16-64.

Cho, C., Jung-Ha, H., Willis, W. D., Goulding, E. H., Stein, P., Xu, Z., Schultz, R. M., Hecht, N. B. and Eddy, E. M. (2003). Protamine 2 deficiency leads to sperm DNA damage and embryo death in mice. *Biol. Reprod.* **69**, 211-217.

Couldrey, C., Carlton, M. B. L., Nolan, P. M., Colledge, W. H. and Evans, M. J. (1999). A retroviral gene trap insertion into the histone 3.3A gene causes partial neonatal lethality, stunted growth, neuromuscular deficits and male sub-fertility in transgenic mice. *Hum. Mol. Genet.* **8**, 2489-2495.

Erkek, S., Hisano, M., Liang, C.-Y., Gill, M., Murr, R., Dieker, J., Schübeler, D., van der Vlag, J., Stadler, M. B. and Peters, A. H. F. M. (2013). Molecular determinants of nucleosome retention at CpG-rich sequences in mouse spermatozoa. *Nat. Struct. Mol. Biol.* **20**, 868-875.

Gaucher, J., Boussouar, F., Montellier, E., Curtet, S., Buchou, T., Bertrand, S., Hery, P., Jounier, S., Depaux, A. and Vitte, A.-L. et al. (2012). Bromodomain-dependent stage-specific male genome programming by Brdt. *EMBO J.* **31**, 3809-3820.

Gaysinskaya, V., Soh, I. Y., van der Heijden, G. W. and Bortvin, A. (2014). Optimized flow cytometry isolation of murine spermatocytes. *Cytometry A* **85**, 556-565.

Getun, I. V., Torres, B. and Bois, P. R. (2011). Flow cytometry purification of mouse meiotic cells. *J. Vis. Exp.* **50**, e2602.

Godmann, M., Auger, V., Ferraroni-Aguiar, V., Di Sauro, A., Sette, C., Behr, R. and Kimmins, S. (2007). Dynamic regulation of histone H3 methylation at lysine 4 in mammalian spermatogenesis. *Biol. Reprod.* **77**, 754-764.

Hake, S. B., Garcia, B. A., Duncan, E. M., Kauer, M., Dellaire, G., Shabanowitz, J., Bazett-Jones, D. P., Allis, C. D. and Hunt, D. F. (2006). Expression patterns and post-translational modifications associated with mammalian histone H3 variants. *J. Biol. Chem.* **281**, 559-568.

Hammoud, S. S., Nix, D. A., Zhang, H., Purwar, J., Carrell, D. T. and Cairns, B. R. (2009). Distinctive chromatin in human sperm packages genes for embryo development. *Nature* **460**, 473-478.

Hess, R. A. and Renato de Franca, L. (2008). Spermatogenesis and cycle of the seminiferous epithelium. *Adv. Exp. Med. Biol.* **636**, 1-15.

Hödl, M. and Basler, K. (2009). Transcription in the absence of histone H3.3. *Curr. Biol.* **19**, 1221-1226.

Huang da, W., Sherman, B. T. and Lempicki, R. A. (2009a). Bioinformatics enrichment tools: paths toward the comprehensive functional analysis of large gene lists. *Nucleic Acids Res.* **37**, 1-13.

Huang da, W., Sherman, B. T. and Lempicki, R. A. (2009b). Systematic and integrative analysis of large gene lists using DAVID bioinformatics resources. *Nat. Protoc.* **4**, 44-57.

Iwamori, N., Zhao, M., Meistrich, M. L. and Matzuk, M. M. (2011). The testis-enriched histone demethylase, KDM4D, regulates methylation of histone H3 lysine 9 during spermatogenesis in the mouse but is dispensable for fertility. *Biol. Reprod.* **84**, 1225-1234.

Jenuwein, T. and Allis, C. D. (2001). Translating the histone code. *Science* **293**, 1074-1080.

Jin, C., Zang, C., Wei, G., Cui, K., Peng, W., Zhao, K. and Felsenfeld, G. (2009). H3.3/H2A.Z double variant-containing nucleosomes mark 'nucleosome-free regions' of active promoters and other regulatory regions. *Nat. Genet.* **41**, 941-945.

Korhonen, H. M., Meikar, O., Yadav, R. P., Papaioannou, M. D., Romero, Y., Da Ros, M., Herrera, P. L., Toppari, J., Nef, S. and Kotaja, N. (2011). Dicer is required for haploid male germ cell differentiation in mice. *PLoS ONE* **6**, e24821.

Kouzarides, T. (2007). Chromatin modifications and their function. *Cell* **128**, 693-705.

Lee, K., Haugen, H. S., Clegg, C. H. and Braun, R. E. (1995). Premature translation of protamine 1 mRNA causes precocious nuclear condensation and arrests spermatid differentiation in mice. *Proc. Natl. Acad. Sci. USA* **92**, 12451-12455.

Lewis, J. D., Abbott, D. W. and Ausió, J. (2003). A haploid affair: core histone transitions during spermatogenesis. *Biochem. Cell Biol.* **81**, 131-140.

Lin, C.-J., Conti, M. and Ramalho-Santos, M. (2013). Histone variant H3.3 maintains a decondensed chromatin state essential for mouse preimplantation development. *Development* **140**, 3624-3634.

Liu, Z., Zhou, S., Liao, L., Chen, X., Meistrich, M. and Xu, J. (2010). Jmjd1a demethylase-regulated histone modification is essential for cAMP-response element modulator-regulated gene expression and spermatogenesis. *J. Biol. Chem.* **285**, 2758-2770.

Martins, R. P. and Krawetz, S. A. (2007). Decondensing the protamine domain for transcription. *Proc. Natl. Acad. Sci. USA* **104**, 8340-8345.

McKittrick, E., Gafken, P. R., Ahmad, K. and Henikoff, S. (2004). Histone H3.3 is enriched in covalent modifications associated with active chromatin. *Proc. Natl. Acad. Sci. USA* **101**, 1525-1530.

Meistrich, M. L. and Hess, R. A. (2013). Assessment of spermatogenesis through staging of seminiferous tubules. *Methods Mol. Biol.* **927**, 299-307.

Miller, D., Brinkworth, M. and Iles, D. (2010). Paternal DNA packaging in spermatozoa: more than the sum of its parts? DNA, histones, protamines and epigenetics. *Reproduction* **139**, 287-301.

Montellier, E., Boussouar, F., Rousseaux, S., Zhang, K., Buchou, T., Fenaille, F., Shiota, H., Debernardi, A., Hery, P. and Curtet, S. et al. (2013). Chromatin-to-nucleoprotamine transition is controlled by the histone H2B variant TH2B. *Genes Dev.* **27**, 1680-1692.

Morales, A., Mohamed, F. and Cavicchia, J. C. (2007). Apoptosis and blood-testis barrier during the first spermatogenic wave in the pubertal rat. *Anat. Rec. (Hoboken)* **290**, 206-214.

Mruk, D. D. and Cheng, C. Y. (2004). Sertoli-Sertoli and Sertoli-germ cell interactions and their significance in germ cell movement in the seminiferous epithelium during spermatogenesis. *Endocr. Rev.* **25**, 747-806.

Nakayama, T., Nishioka, K., Dong, Y.-X., Shimojima, T. and Hirose, S. (2007). Drosophila GAGA factor directs histone H3.3 replacement that prevents the heterochromatin spreading. *Genes Dev.* **21**, 552-561.

Oishi, K., Barchi, M., Au, A. C., Gelb, B. D. and Diaz, G. A. (2004). Male infertility due to germ cell apoptosis in mice lacking the thiamin carrier, Tht1. A new insight into the critical role of thiamin in spermatogenesis. *Dev. Biol.* **266**, 299-309.

Okada, Y., Scott, G., Ray, M. K., Mishina, Y. and Zhang, Y. (2007). Histone demethylase JHDM2A is critical for Tnp1 and Prm1 transcription and spermatogenesis. *Nature* **450**, 119-123.

O'Carroll, D., Scherthan, H., Peters, A. H. F. M., Opravil, S., Haynes, A. R., Laible, G., Rea, S., Schmid, M., Lebersorger, A. and Jerratsch, M. et al. (2000). Isolation and characterization of Suv39h2, a second histone H3 methyltransferase gene that displays testis-specific expression. *Mol. Cell. Biol.* **20**, 9423-9433.

Payne, C. and Braun, R. E. (2006). Histone lysine trimethylation exhibits a distinct perinuclear distribution in Plzf-expressing spermatogonia. *Dev. Biol.* **293**, 461-472.

Peters, A. H. F. M., O'Carroll, D., Scherthan, H., Mechtler, K., Sauer, S., Schöfer, C., Weipoltshammer, K., Pagani, M., Lachner, M. and Kohlmaier, A. et al. (2001). Loss of the Suv39h histone methyltransferases impairs mammalian heterochromatin and genome stability. *Cell* **107**, 323-337.

Rathke, C., Baarends, W. M., Awe, S. and Renkawitz-Pohl, R. (2013). Chromatin dynamics during spermiogenesis. *Biochim. Biophys. Acta* **1839**, 155-168.

Ray-Gallet, D., Woolfe, A., Vassias, I., Pellentz, C., Lacoste, N., Puri, A., Schultz, D. C., Pchelintsev, N. A., Adams, P. D. and Jansen, L. E. et al. (2011). Dynamics of histone H3 deposition in vivo reveal a nucleosome gap-filling mechanism for H3.3 to maintain chromatin integrity. *Mol. Cell* **44**, 928-941.

Sakai, A., Schwartz, B. E., Goldstein, S. and Ahmad, K. (2009). Transcriptional and developmental functions of the H3.3 histone variant in Drosophila. *Curr. Biol.* **19**, 1816-1820.

Szasz, F., Sirivaidyapong, S., Cheng, F. P., Voorhout, W. F., Marks, A., Colenbrander, B. and Solti, B. M. (2000). Detection of calcium ionophore induced membrane changes in dog sperm as a simple method to predict the cryopreservability of dog semen. *Mol. Reprod. Dev.* **55**, 289-298.

Szenker, E., Ray-Gallet, D. and Almouzni, G. (2011). The double face of the histone variant H3.3. *Cell Res.* **21**, 421-434.

Tachibana, M., Nozaki, M., Takeda, N. and Shinkai, Y. (2007). Functional dynamics of H3K9 methylation during meiotic prophase progression. *EMBO J.* **26**, 3346-3359.

Tagami, H., Ray-Gallet, D., Almouzni, G. and Nakatani, Y. (2004). Histone H3.1 and H3.3 complexes mediate nucleosome assembly pathways dependent or independent of DNA synthesis. *Cell* **116**, 51-61.

Tan, M., Luo, H., Lee, S., Jin, F., Yang, J. S., Montellier, E., Buchou, T., Cheng, Z., Rousseaux, S. and Rajagopal, N. et al. (2011). Identification of 67 histone marks and histone lysine crotonylation as a new type of histone modification. *Cell* **146**, 1016-1028.

Tang, M. C. W., Jacobs, S. A., Wong, L. H. and Mann, J. R. (2013). Conditional allelic replacement applied to genes encoding the histone variant H3.3 in the mouse. *Genesis* **51**, 142-146.

van der Heijden, G. W., Derijck, A. A. H. A., Ramos, L., Giele, M., van der Vlag, J. and de Boer, P. (2006). Transmission of modified nucleosomes from the mouse male germline to the zygote and subsequent remodeling of paternal chromatin. *Dev. Biol.* **298**, 458-469.

van der Heijden, G. W., Derijck, A. A. H. A., Pósfai, E., Giele, M., Pelczar, P., Ramos, L., Wansink, D. G., van der Vlag, J., Peters, A. H. F. M. and de Boer, P. (2007). Chromosome-wide nucleosome replacement and H3.3 incorporation during mammalian meiotic sex chromosome inactivation. *Nat. Genet.* **39**, 251-258.

Witt, O., Albig, W. and Doenecke, D. (1997). Transcriptional regulation of the human replacement histone gene H3.3B. *FEBS Lett.* **408**, 255-260.

Yu, Y. E., Zhang, Y., Unni, E., Shirley, C. R., Deng, J. M., Russell, L. D., Weil, M. M., Behringer, R. R. and Meistrich, M. L. (2000). Abnormal spermatogenesis and reduced fertility in transition nuclear protein 1-deficient mice. *Proc. Natl. Acad. Sci. USA* **97**, 4683-4688.

Zhao, M., Shirley, C. R., Mounsey, S. and Meistrich, M. L. (2004). Nucleoprotein transitions during spermiogenesis in mice with transition nuclear protein Tnp1 and Tnp2 mutations. *Biol. Reprod.* **71**, 1016-1025.

Zheng, J., Xia, X., Ding, H., Yan, A., Hu, S., Gong, X., Zong, S., Zhang, Y. and Sheng, H. Z. (2008). Erasure of the paternal transcription program during spermiogenesis: the first step in the reprogramming of sperm chromatin for zygotic development. *Dev. Dyn.* **237**, 1463-1476.

DEVELOPMENT